η^6-(2-Phenoxyethanol) ruthenium(II)-complexes of 2,2'-bipyridine and its derivatives: solution speciation and kinetic behaviour

Guilherme Nogueira[a], Orsolya Dömötör[b,c], Adhan Pilon[a], M. Paula Robalo[d,e], Fernando Avecilla[f], M. Helena Garcia[a], Éva A. Enyedy[c,*], Andreia Valente[a,*]

[a]Centro de Química Estrutural, Faculdade de Ciências da Universidade de Lisboa, Campo Grande, 1749-016 Lisboa, Portugal.

[b]MTA-SZTE Bioinorganic Chemistry Research Group, University of Szeged, Dóm tér 7, H-6720 Szeged, Hungary

[c]Department of Inorganic and Analytical Chemistry, University of Szeged, Dóm tér 7, H-6720 Szeged, Hungary

[d]Área Departamental de Engenharia Química, Instituto Superior de Engenharia de Lisboa, Rua Conselheiro Emídio Navarro 1, 1959-007 Lisboa, Portugal.

[e]Centro de Química Estrutural, Instituto Superior Técnico, Universidade de Lisboa, Av. Rovisco Pais, 1049-001 Lisboa, Portugal.

[f]Departamento de Química Fundamental, Universidade da Coruña, Campus de A, Zapateria 15071, A Coruña, Spain.

1

STRUCTURES and ABBREVIATIONS

1 $[Ru^{II}(\eta^6\text{-}(2\text{-phenoxyethanol}))(\mu^2\text{-Cl})Cl]_2$

2 $[Ru^{II}(\eta^6\text{-}(2\text{-phenoxyethanol}))(NCCH_3)_2Cl][PF_6]$

3 $[Ru^{II}(\eta^6\text{-}(2\text{-phenoxyethanol}))(2,2'\text{-bipyridine})Cl][PF_6]$

4 $[Ru^{II}(\eta^6\text{-}(2\text{-phenoxyethanol}))(4,4'\text{-dimethyl-}2,2'\text{-bipyridine})Cl][PF_6]$

5 $[Ru^{II}(\eta^6\text{-}(2\text{-phenoxyethanol}))(4,4'\text{-diyldimethanol-}2,2'\text{-bipyridine})Cl][PF_6]$

bpy   2,2'-bipyridine

PBS   phosphate buffered saline

PBS'   modified phosphate buffered saline

ABSTRACT

A novel family of Ru^{II}-arene compounds with the general formula of $[Ru^{II}(\eta^6\text{-}(2\text{-phenoxyethanol}))(L)Cl]^+$ (L: 2,2'-bipyridine (bpy) (**3**), 4,4'-dimethyl-2,2'-bipyridine (**4**) and 4,4'-diyldimethanol-2,2'-bipyridine (**5**)) was synthesized and characterized by standard spectroscopic and analytical methods. Complex **3** was further studied by single-crystal X-ray diffraction analysis, showing a pseudo octahedral geometry and strong π-π lateral stacking interactions in the crystal packing. Effect of the substituents on the electrochemical properties and on the aqueous solution stability was monitored by cyclic voltammetry, UV–Vis and ^{1}H NMR spectroscopy. Complexes **3-5** presented multiple irreversible redox processes according to their cyclic voltammograms recorded in acetonitrile, and their $Ru^{II} \rightarrow Ru^{III}$ oxidation peaks were found at *ca.* +1.6 V. Hydrolysis of the binuclear $[Ru^{II}(\eta^6\text{-}(2\text{-phenoxyethanol}))(\mu^2\text{-Cl})Cl]_2$ precursor (**1**) resulted in binuclear hydroxido bridged species $[(Ru^{II}(\eta^6\text{-}(2\text{-phenoxyethanol})))_2(\mu\text{-OH})_3]^+$ and $[(Ru^{II}(\eta^6\text{-}(2\text{-phenoxyethanol})))_2(\mu\text{-}$

OH)$_2$Z$_2$] (Z = H$_2$O/Cl$^-$) in the presence of chloride ions in water. The hydrolytic behaviour of this Ru^{II} precursor is similar to that of the analogous species [Ru^{II}(η^6-p-cymene)(μ^2-Cl)Cl]$_2$ regarding the hydrolysis products and their stability constants. Formation of complexes **3-5** by reaction of the Ru^{II} precursor with the (N,N) bidentate ligands was found to be relatively slow in aqueous solution. The complexation is complete already at pH 1 due to the formation of [Ru^{II}(η^6-(2-phenoxyethanol))(L)Z] complexes of significantly high stability in all cases, which are predominant species up to pH 6. However, besides the formation of the mixed hydroxido species [Ru^{II}(η^6-(2-phenoxyethanol))(L)(OH)]$^+$ at neutral and basic pH values, the slow oxidation of the Ru^{II} centre takes place as well leading to the partial loss of the arene moiety. The rate of these processes depends on the pH and its maximum was found at pH 8-9. Additionally the chlorido/aqua co-ligand exchange processes of the [Ru^{II}(η^6-(2-phenoxyethanol))(L)Cl]$^+$ species were also monitored and only ~5% of the chlorido ligand was found to be replaced by water in 0.1 M chloride ion containing aqueous solutions at pH 5.

1. Introduction

During the last two decades a significant amount of work has been published in the field of ruthenium metallodrugs for application as anticancer agents due to the relevant cytotoxicity exhibited by many of these compounds against several cancer cell lines [1-5]. Particular attention has been given to the families of the so called piano-stool geometries where the stool is formed by the 'η^5-C$_5$H$_5$' or 'η^6-C$_6$H$_6$' bonded to the ruthenium centre and the three legs are represented by sigma coordinated ligands. These arene ligands, besides stabilization of the Ru^{II} centre, also provide a hydrophobic core for the complex which is an important feature for biomolecular recognition processes and transport of ruthenium through cell membranes.

Representative structures of '(η^5-C_5H_5)-Ru' are [Ru^{II}(η^5-C_5H_5)(PPh$_3$)(2,2'-bipyridine][CF$_3$SO$_3$], TM34, and other related structures with (N,N) and (N,O) bidentate ligands as non-leaving groups and triphenylphosphane as the mono coordinated ligand [6-10]. Representative structures of '(η^6-C_6H_6)-Ru' are the so called RAPTA and RM-complexes [11]. RAPTA complexes present a phosphoadamantane as non-leaving group with two chloride atoms playing the role of leaving ligands [12]. RM-complexes possess the bidentate ethylenediamine as non-leaving group and one chlorido ligand prompt for aquation [13]. The importance as potential anticancer agents of compounds of general formula [Ru^{II}(η^6-arene)(N,N)Cl]$^+$ lead to extensive studies comprising the variation of the arene group and the (N,N) bidentate ligand [14-19,20]. In these studies the η^6-arene ligand has been thoroughly chosen as *p*-cymene, benzene, 2-phenylethanol, indane, phenylpropanoids, hexamethylbenzene or biphenyl. A variety of (N,N) bidentate ligands such as 4-anilinoquinazolines, naphthalimide tethered chelating ligands, ethylenediamine, bipyridine, 2-diaminobenzene, *o*-phenylenediamine, *o*-benzoquinonediimine, azopyridines, among others, was tested [14-19,20]. The mechanism of action for the generality of compounds from this family has been related as expected, to the lability of the chlorido ligand due to its hydrolysis in aqueous environment [20-22]. The rate and extend for these aquation reactions are influenced by both the different physiological conditions, such as the pH and the concentration of the chloride ions [15,19,20,23], as well as the nature of the coordinated (N,N) ligand and only little influence was noticed for the η^6-arene ligands [16,23]. Interestingly, it was found that half-lives for aquation can vary from some minutes when (N,N) are 4-anilinoquinazoline ligands to several hours in the case of azopyridine ligands [16,20].

Our approach to get through this subject was to understand the role of different (N,N) co-ligands on the reactivity of the less studied fragment {$Ru^{II}(\eta^6$-(2-phenoxyethanol))Cl}$^+$. For this purpose different substituents (R) were introduced in the basic 2,2'-bipyridine (bpy) structure giving the (bpy-R) following ligands: bpy (R = H), 4,4'-dimethyl-2,2'-bipyridine (R = methyl) and 4,4'-diylmethanol-2,2'-bipyridine (R = methanol). Thus, a new family of compounds presenting the general formula [$Ru^{II}(\eta^6$-(2-phenoxyethanol))(bpy-R)Cl]$^+$ was synthesized and fully characterized by the usual methods such as spectroscopic and electrochemical techniques and the structure of one of the new compounds was also complemented by single crystal X-ray diffraction studies. The influence of the substitution of these bidentate ligands on the hydrolysis of the three newly synthesized complexes was studied in aqueous solution by the combined use of UV–Vis and ^{1}H NMR titrations in several experimental conditions.

2. Experimental

2.1. General procedures

Bpy, 4,4'-dimethyl-2,2'-bipyridine, KCl, NaCl, Na_2HPO_4, KH_2PO_4, KNO_3, $AgNO_3$, HCl, HNO_3 and KOH were purchased from Sigma-Aldrich and used without further purification. 4,4'-Diylmethanol-2,2'-bipyridine was purchased from Carbosynth and used without further purification. All solvents were analytical or reagent grade. All syntheses were carried out under dinitrogen atmosphere using current *Schlenk* techniques and the solvents used were dried using standard methods [24]. The doubly purified water was obtained from a Miliipore® system. Dimeric [$Ru^{II}(\eta^6$-(2-phenoxyethanol))(μ^2-Cl)Cl]$_2$ (**1**) and [$Ru^{II}(\eta^6$-(2-phenoxyethanol))(NCCH$_3$)$_2$Cl][PF$_6$] (**2**) starting materials were prepared according to the methods described in literature [25,26]. FT-IR spectra were recorded in a Shimadzu

IRAffinity-1 FTIR spectrophotometer with KBr; only significant bonds are cited in text. ^{1}H-, ^{13}C- and ^{31}P-NMR spectra were recorded on a Bruker Avance 400 spectrometer at probe temperature (for chemical characterization). Chemical shifts (*s* = singlet; *d* = duplet; *m* = multiplet for ^{1}H) are reported in parts per million (ppm) downfield from internal Me$_4$Si standards. For the titration measurements, a Bruker Ultrashield 500 Plus instrument was used, using 4,4-dimethyl-4-silapentane-1-sulfonic acid as an internal NMR standard. Data acquisition and treatment were performed using TopSpin 3.2 (Brucker NMR software). Elemental analyses were obtained at *Laboratório de Análises, Instituto Superior Técnico*, using Fisons Instruments EA1108 system. Data acquisition, integration and handling were performed with EAGER-200 software package (Carlo Erba Instrumets). Electronic spectra were recorded at room temperature on a Jasco V-660 spectrometer in the range of 200-900 nm, using quartz cells with 1 cm width (for chemical characterization) or on a Thermo Scientific Evolution 220 spectrophotometer in the interval 200-850 nm (for titration measurements). The path length in this case was 1 or 0.5 cm.

2.2. Complexes syntheses

<u>Synthesis of complex 3:</u> [Ru^{II}(η^6-(2-phenoxyethanol))(bpy)Cl][PF$_6$]

To a stirred solution of [Ru^{II}(η^6-(2-phenoxyethanol))(NCCH$_3$)$_2$Cl][PF$_6$] (250 mg, 0.50 mmol) in acetonitrile (25 mL), bpy (100 mg, 0.65 mmol) was added. After stirring for 6 h at room temperature, the reaction mixture was filtered and the solvent was evaporated under vacuum, yielding an orange powder that was recrystallized twice from CH$_3$CN/diethylether (Et$_2$O) to afford **3** as small orange crystals needle-shaped.

Yield: 77%. FTIR (KBr, cm^{-1}): ν(C-H aromatic) 3140-3000, ν(C=C aromatic) 1620 and 1537, ν(C-H aliphatic) 3000-2850, ν(O-H) 3650-3250, ν(C-O) 1282, ν(C-N) 1250-1000, ν(PF$_6^-$) 844 and 557. ^{1}H-RMN [CD$_3$CN, Me$_4$Si, δ/ppm (multiplicity, integration, assignment)]: 9.34 (d, 2,

H$_1$, $^3J_{HH}$ = 5.3 Hz), 8.31 (d, 2, H$_4$, $^3J_{HH}$ = 8.1 Hz), 8.16 (t, 2, H$_3$, $^3J_{HH}$ = 7.9 Hz), 7.68 (t, 2, H$_2$, $^3J_{HH}$ = 6.6 Hz), 6.21 (t, 2, H$_{meta\text{-arene}}$, $^3J_{HH}$ = 6.0 Hz), 5.51 (d, 2, H$_{ortho\text{-arene}}$, $^3J_{HH}$ = 6.4 Hz), 5.42 (t, 1, H$_{para\text{-arene}}$, $^3J_{HH}$ = 5.5 Hz), 4.12 (t, 2, -O-C**H$_2$**-, $^3J_{HH}$ = 4.4 Hz), 3.78 (m, 2, -**CH$_2$**OH), 3.22 (t, 1, -O**H**, $^3J_{HH}$ = 5.8 Hz). ^{13}C-RMN [CD$_3$CN, δ/ppm]: 156.0 (C$_1$), 155.8 (C$_5$), 140.6 (C$_3$), 140.2 (C$_{q\text{-arene}}$), 128.2 (C$_2$), 124.4 (C$_4$), 95.8 (C$_{meta\text{-arene}}$), 73.9 (C$_{para\text{-arene}}$), 72.9 (-O-**CH$_2$**-), 65.8 (C$_{ortho\text{-arene}}$), 60.5 (-**CH$_2$**OH). ^{31}P-RMN [CD$_3$CN, δ/ppm]: -144.65 (septuplet, PF$_6^-$). UV-Vis [CH$_3$CN, λ$_{max}$ / nm (ε / M^{-1} cm^{-1})]: 204 (31926), 237 (18551), 290 (17037), 304 (*Sh*), 314 (11951), 349 (3282), 412 (*Sh*). Elemental analysis (%) Found: C 37.6, H 3.0, N 5.1. Calc. for C$_{18}$H$_{18}$ClF$_6$N$_2$O$_2$PRu•0.1CH$_3$CN: C 37.7, H 3.2, N 5.1.

Synthesis of complex 4: [Ru^{II}(η^6-(2-phenoxyethanol))(4,4'-dimethyl-2,2'-bipyridine)Cl][PF$_6$]

4,4'-dimethyl-2,2'-bypiridine (60 mg, 0.33 mmol) was added to a stirred solution of [Ru^{II}(η^6-C$_6$H$_5$OCH$_2$CH$_2$OH)(NCCH$_3$)$_2$Cl][PF$_6$] (150 mg, 0.30 mmol) in acetonitrile (20 ml). The reaction mixture was stirred for 6 h at room temperature and then filtrated. The solution was evaporated, yielding **4** as small orange crystals needle-shaped after two recrystallizations from CH$_3$CN/Et$_2$O.

Yield: 73%. FTIR (KBr, cm^{-1}): ν(C-H aromatic) 3140-3000, ν(C=C aromatic) 1620 and 1529, ν(C-H aliphatic) 3000-2850, ν(O-H) 3650-3250, ν(C-O) 1276, ν(C-N) 1250-1000, ν(PF$_6^-$) 835 and 557. ^{1}H-RMN (CD$_3$CN, Me$_4$Si, δ/ppm [multiplicity, integration, assignment]): 9.14 (d, 2, H$_1$, $^3J_{HH}$ = 5.8 Hz), 8.15 (s, 2, H$_4$), 7.50 (d, 2, H$_2$, $^3J_{HH}$ = 5.6 Hz), 6.17 (t, 2, H$_{meta\text{-arene}}$, $^3J_{HH}$ = 6.0 Hz), 5.48 (d, 2, H$_{ortho\text{-arene}}$, $^3J_{HH}$ = 6.4 Hz), 5.37 (t, 1, H$_{para\text{-arene}}$, $^3J_{HH}$ = 5.6 Hz), 4.11 (t, 2, -O-C**H$_2$**-, $^3J_{HH}$ = 4.4 Hz), 3.78 (m, 2, -**CH$_2$**OH), 3.22 (m, 1, -O**H**), 2.57 (s, 6, H$_6$). ^{13}C-RMN [CD$_3$CN, δ/ppm]: 155.4 (C$_5$), 155.1 (C$_1$), 153.3 (C$_3$), 139.8 (C$_{q\text{,arene}}$), 129.0 (C$_2$), 125.0 (C$_4$), 95.4 (C$_{meta\text{-arene}}$), 73.7 (C$_{para\text{-arene}}$), 72.8 (-O-**CH$_2$**-), 65.6 (C$_{ortho\text{-arene}}$), 60.6 (-**CH$_2$**OH), 21.3 (C$_6$).

^{31}P-RMN [CD$_3$CN, δ/ppm]: -144.62 (septuplet, PF$_6^-$). UV-Vis [CH$_3$CN, λ_{max} / nm (ϵ / M^{-1} cm^{-1})]: 208 (31150), 237 (*Sh*), 287 (13095), 303 (*Sh*), 311 (*Sh*), 346 (2773), 413 (*Sh*). Elemental analysis (%) Found: C 39.8, H 3.7, N 4.6. Calc. for C$_{20}$H$_{22}$ClF$_6$N$_2$O$_2$PRu: C 39.8, H 3.7, N 4.6.

Synthesis of complex 5: [Ru^{II}(η^6-(2-phenoxyethanol))(4,4'-diyldimethanol-2,2'-bipyridine)Cl][PF$_6$]

To a stirred solution of [Ru^{II}(η^6-(2-phenoxyethanol))(NCCH$_3$)$_2$Cl][PF$_6$] (208 mg, 0.41 mmol) in acetonitrile (20 ml) was added (4,4'-diyldimethanol-2,2'-bipyridine) (94 mg, 0.46 mmol). After stirring for 4 h at 40ºC, Celite$^®$ 521 was added and the mixture was stirred for 15 min and cannula-filtrated. Then the solvent was evaporated, the product was dissolved in water, filtrated and evaporated. Finally, the product was recrystallized from CH$_3$CN/Et$_2$O yielding **5** as a yellow powder.

Yield: 55%. FTIR (KBr, cm^{-1}): ν(C-H aromatic) 3140-3000, ν(C=C aromatic) 1620 and 1529, ν(C-H aliphatic) 3000-2850, ν(O-H) 3700-3150, ν(C-O) 1273, ν(C-N) 1250-1000, ν(PF$_6^-$) 844 and 559. ^{1}H-RMN (CD$_3$CN, Me$_4$Si, δ/ppm [multiplicity, integration, assignment]): 9.24 (d, 2, H$_1$, $^3J_{HH}$ = 5.8 Hz), 8.29 (s, 2, H$_4$), 7.63 (d, 2, H$_2$, $^3J_{HH}$ = 5.7 Hz), 6.20 (t, 2, H$_{meta\text{-}arene}$, $^3J_{HH}$ = 5.8 Hz), 5.49 (d, 2, H$_{ortho\text{-}arene}$, $^3J_{HH}$ = 6.3 Hz), 5.40 (t, 1, H$_{para\text{-}arene}$, $^3J_{HH}$ = 5.4 Hz), 4.84 (s, 4, H$_6$), 4.11 (t, 2, -O-C**H**$_2$-, $^3J_{HH}$ = 4.4 Hz), 3.78 (m, 3, -C**H**$_2$OH + O**H**,bpy), 3.24 (m, 1, -O**H**,arene). ^{1}H-RMN (DMSO-d$_6$, Me$_4$Si, δ/ppm [multiplicity, integration, assignment]): 9.44 (d, 2, H$_1$, $^3J_{HH}$ = 5.6 Hz), 8.48 (s, 2, H$_4$), 7.69 (d, 2, H$_2$, $^3J_{HH}$ = 5.6 Hz), 6.38 (t, 2, H$_{meta\text{-}arene}$, $^3J_{HH}$ = 5.8 Hz), 5.81 (d, 4, H$_{ortho\text{-}arene}$+O**H**,bpy), 5.56 (t, 1, H$_{para\text{-}arene}$, $^3J_{HH}$ = 5.2 Hz), 4.78 (d, 4, H$_6$, $^3J_{HH}$ = 5.1 Hz), 4.08 (t, 2, -O-C**H**$_2$-, $^3J_{HH}$ = 4.4 Hz), 3.68 (m, 2, -C**H**$_2$OH,arene). ^{13}C-RMN [DMSO-d$_6$, δ/ppm]: 156.2 (C$_3$), 154.9 (C$_1$), 154.2 (C$_5$), 138.7 (C$_{q,arene}$), 124.2 (C$_2$), 120.3 (C$_4$), 94.5 (C$_{meta\text{-}arene}$), 72.7 (C$_{para\text{-}arene}$), 71.5 (-O-**C**H$_2$-), 64.5 (C$_{ortho\text{-}arene}$), 61.1 (C$_6$), 58.9 (-**C**H$_2$OH).

^{31}P-RMN [DMSO-d$_6$, δ/ppm]: -144.22 (septuplet, PF$_6^-$). UV-Vis [CH$_3$CN, λ$_{max}$ / nm (ε / M^{-1} cm^{-1})]: 208 (40723), 234 (*Sh*), 287 (13337), 303 (*Sh*), 311 (*Sh*), 346 (2848), 413 (*Sh*). Elemental analysis (%) Found: C 37.8, H 3.5, N 4.4. Calc. for C$_{20}$H$_{22}$ClF$_6$N$_2$O$_4$PRu: C 37.8, H 3.4, N 4.4.

2.3. X-ray crystal structure determination

Three-dimensional X-ray data for complex **3** were collected on a Bruker SMART Apex CCD diffractometer at 100(2) K, using a graphite monochromator and Mo-K_α radiation (λ = 0.71073 Å) by the ϕ-ω scan method. Reflections were measured from a hemisphere of data collected of frames, each of them covering 0.3 degrees in ω. A total of 35340 reflections measured for **3** were corrected for Lorentz and polarization effects and for absorption by semi-empirical methods based on symmetry-equivalent and repeated reflections. Of the total, 5806 independent reflections exceeded the significance level $|F|/\sigma(|F|) > 4.0$. After data collection, in each case an multi-scan absorption correction (SADABS) [27] was applied, and the structure was solved by direct methods and refined by full matrix least-squares on F^2 data using SHELX suite of programs [28]. Refinements were done with allowance for thermal anisotropy of all non-hydrogen atoms. The hydrogen atoms were located in difference Fourier map and freely refined, except for O(1), C(1), C(2A) and C(2B), which were included in calculation position and refined in the riding mode. A final difference Fourier map showed no residual density outside: 0.804 and -0.879 e.Å^{-3} for **3**. A weighting scheme w = 1/[σ^2(F$_o^2$) + (0.018200 P)^2 + 2.988100P] for **3**, where P = ($|F_o|^2$ + 2$|F_c|^2$)/3, were used in the latter stages of refinement. The crystal presents important disorder on the ethanol group of the 2-phenoxyethanol. The disorder on ethanol group was resolved and the atomic sites have been observed and refined with anisotropic atomic displacement parameters. The site occupancy factor was 0.76731 for O(2A) and C(2A). CCDC 1479923 contains the supplementary

crystallographic data for the structure reported in this paper. These data can be obtained free of charge via http://www.ccdc.cam.ac.uk/conts/retrieving.html, or from the Cambridge Crystallographic Data Centre, 12 Union Road, Cambridge CB2 1EZ, UK; fax: (+44) 1223 336 033; or e-mail: deposit@ccdc.cam.ac.uk. Supplementary data associated with this article can be found, in the online version, at doi: $$$$$. Crystal data and details of the data collection and refinement for the new compounds are collected in Table S1.

2.4. Electrochemical studies

The electrochemical experiments were performed on an EG&G Princeton Applied Research Model 273A potentiostat/galvanostat and monitored with the Electrochemistry PowerSuite v2.51 software from Princeton Applied Research. Cyclic voltammograms of the complexes (1.0×10^{-3} M) were obtained in 0.1 M solutions of $[NBu_4][PF_6]$ in $NCCH_3$, using a three-electrode configuration cell with a platinum-disk working electrode (1.0 mm diameter) probed by a Luggin capillary connected to a silver-wire pseudo-reference electrode and a Pt wire counter electrode. The electrochemical experiments were performed under a dinitrogen atmosphere at room temperature. The redox potentials were measured in the presence of ferrocene as the internal standard and the redox potential values are normally quoted relative to the SCE by using the ferrocenium/ferrocene redox couple ($E_{1/2}$ = +0.40 V *vs*. SCE for $NCCH_3$). The supporting electrolyte was purchased from Fluka (electrochemical grade), dried under vacuum for several hours and used without further purification. Reagent grade acetonitrile and dichloromethane were dried over P_2O_5 and CaH_2, respectively and distilled under dinitrogen atmosphere before use.

2.5. UV–Vis spectrophotometric and ^1H NMR titration measurements

2.5.1. Preparation of complex solutions

A stock solution of $[Ru^{II}(\eta^6\text{-(2-phenoxyethanol)})Z_3]$ (where Z = H_2O and/or Cl^-; charges are omitted for simplicity) was obtained by dissolving a known amount of the dimeric precursor $[Ru^{II}(\eta^6\text{-(2-phenoxyethanol)})(\mu^2\text{-Cl})Cl]_2$ **1** in water. The chloride ion free complex $[Ru^{II}(\eta^6\text{-(2-phenoxyethanol)})(H_2O)_3]^{2+}$ was prepared by the addition of equivalent amount of $AgNO_3$ to the dissolved **1** and AgCl precipitate was removed by filtration. The complexes **2–5** were dissolved in pure water and the stock solutions were kept in freezer or in 0.005 M HCl (pH ~ 2.5) and the final solutions were kept in fridge. For measurements performed at pH 7.40 a modified phosphate buffered saline buffer (PBS') was applied: 100.5 mM NaCl, 1.5 mM KCl, 12.0 mM Na_2HPO_4, 3.0 mM KH_2PO_4 in which the concentration of the K^+, Na^+ and Cl^- ions corresponds to that of the human blood serum.

2.5.2. Measurements

The spectrophotometric titrations were performed on samples containing the bpy-R free ligands (200 μM); $[Ru^{II}(\eta^6\text{-(2-phenoxyethanol)})Z_3]$ (200 μM) or the metal complexes **2-5** (138 or 268 μM) over the pH range between 2.0 and 11.5 at an ionic strength of 0.10 M (KCl) in water at 25.0 ± 0.1 °C. Stability constants for the hydrolysis of $[Ru^{II}(\eta^6\text{-(2-phenoxyethanol)})Z_3]$ were calculated with the computer program PSEQUAD [29]. Measurement on the complex **3** was also carried out by preparing individual samples, in which the 0.1 M KCl was partially or completely replaced by HCl to keep the ionic strength constant. Then the pH values, varying in the range ca. 1.0–2.0, were calculated from the strong acid content of the samples since under the applied conditions (low concentration of the complex) the contribution of other species besides HCl to the total $[H^+]$ is negligible. Time dependent measurements were carried out at various pH values using 100–200 μM complex concentrations, and PBS' or 20 mM phosphate solution was used for buffering media at pH 7.40. UV–Vis spectra were also recorded to study the H_2O/Cl^- exchange

equilibrium processes in the [Ru^{II}(η^6-(2-phenoxyethanol))(L)Z] complexes between pH 4.9–5.2 in dependence of the Cl$^-$ concentration (0.2 – 150 mM). Equilibrium constants for this exchange process were calculated with the computer program PSEQUAD [29].

For ^{1}H NMR solution studies the [Ru^{II}(η^6-(2-phenoxyethanol))(μ^2-Cl)Cl]$_2$ **1** was dissolved in a 10% (v/v) D$_2$O/H$_2$O mixture to yield a concentration of 2 mM and was titrated at 25 °C, at *I* = 0.10 M (KCl). Hydrolysis and subsequent oxidation of complex **3** were followed at pH 7.40 in PBS' buffer.

3. Results and discussion

3.1 Synthesis of [Ru^{II}(η^6-(2-phenoxyethanol))(bpy-R)Cl][PF$_6$] complexes

Mononuclear complexes of the general formula [Ru^{II}(η^6-(2-phenoxyethanol))(bpy-R)Cl][PF$_6$] with bpy-R = bpy (**3**), 4,4'-dimethyl-2,2'-bipyridine (**4**) and 4,4'-diylmethanol-2,2'-bipyridine (**5**) were prepared, as shown in Scheme 1, by ligand substitution from the parent cationic complex [Ru^{II}(η^6-(2-phenoxyethanol))(NCCH$_3$)$_2$Cl][PF$_6$] **2** in acetonitrile, at room temperature, in the presence of a slight excess of the corresponding ligand. The new compounds were recrystallized by slow diffusion of diethyl ether in acetonitrile giving crystalline orange to yellow compounds in good yields (55-77%).

The formulation and purity of all the new compounds is supported by analytical data obtained by means of FT-IR spectroscopy, ^{1}H, ^{13}C, ^{31}P NMR spectroscopy and elemental analyses. The solid state FT-IR spectra (KBr pellets) of the complexes presented the characteristic bands of the η^6-(2-phenoxyethanol) moiety ($v_{C-H, \text{stretching}} \sim 3120$ cm^{-1} and $v_{O-H, \text{stretching}} \sim 3500$ cm^{-1}), the bpy-R ligands (*ca.* 1520-1400 cm^{-1}) and the PF$_6^-$ anion ($\sim$ 840 and 560 cm^{-1}) in all the studied complexes. Comparing with the precursor **2**, one can also observe the disappearance of the $v_{C\equiv N, \text{stretching}}$ at $\sim$ 2330 cm^{-1}, as consequence of their replacement by bpy-R.
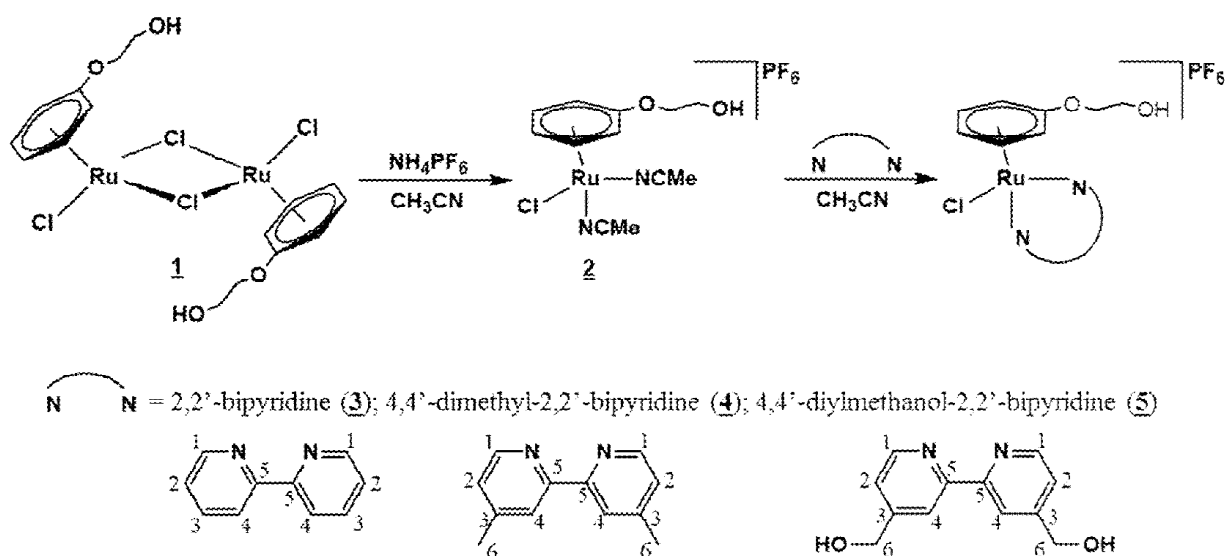
Scheme 1. Reaction scheme for the synthesis of the new [Ru^{II}(η^6-(2-phenoxyethanol))(bpy-R)Cl][PF$_6$] complexes and the structures of the ligands numbered for NMR assignments.

Analysis of the overall ^{1}H NMR data in CD$_3$CN or DMSO-d$_6$, presented on the experimental section, showed that, comparing with [Ru^{II}(η^6-(2-phenoxyethanol))(NCCH$_3$)$_2$Cl][PF$_6$] **2**, the substitution of the acetonitrile ligands by bpy-R did not lead to significant changes on the (de)shielding of the η^6-(2-phenoxyethanol) protons. For all the compounds the η^6-(2-phenoxyethanol) ring displayed signals in the characteristic range of η^6-arene ruthenium(II) compounds ($\approx$ 5.4-6.2 ppm). In all cases, the bipyridine protons of the complexes are more deshielded compared to the free ligands (e.g. $\Delta H_1 \approx 0.65$ ppm, $\Delta H_2 \approx 0.30$ ppm and $\Delta H_3 \approx$ 0.30 ppm for compound **3**) revealing the nature of the σ dative the coordination to the ruthenium centre. The *para* substitution on the bipyridine ring for compounds **4** and **5** also lead to a deshielding on methyl ($\Delta \approx 0.41$ ppm) or hydroxymethyl group (-**CH$_2$OH** $\Delta \approx$ 0.21 ppm) signals, respectively, showing the electronic flow towards these rings. Analysis of the ^{13}C NMR reveals a similar pattern. ^{31}P NMR shows the presence of the PF$_6^-$ counter-ion as a septuplet at −144 ppm.

3.2. UV-visible (UV-Vis) characterization in acetonitrile

Optical absorption spectra of the new complexes **3-5** together with all ligands and precursors (**1**, **2**) were recorded in 10^{-6} - 10^{-3} M acetonitrile solutions (see Experimental Section). Fig. 1 shows the spectra of compounds **3-5** in acetonitrile. All the studied complexes showed intense bands in the UV region attributed to π-π* electronic transitions occurring in the organometallic fragment {Ru^{II}(η^6-(2-phenoxyethanol))Cl}$^+$ (λ ~ 220-260 nm) and in the coordinated chromophores (λ ~ 260 - 400 nm). Additional charge transfer (CT) bands were also observed for all studied complexes. In fact, all complexes presented one band compatible with a MLCT nature from Ru 4d orbitals to the δ symmetry orbitals of the η^6-(2-phenoxyethanol) ring (λ ≈ 413 nm).
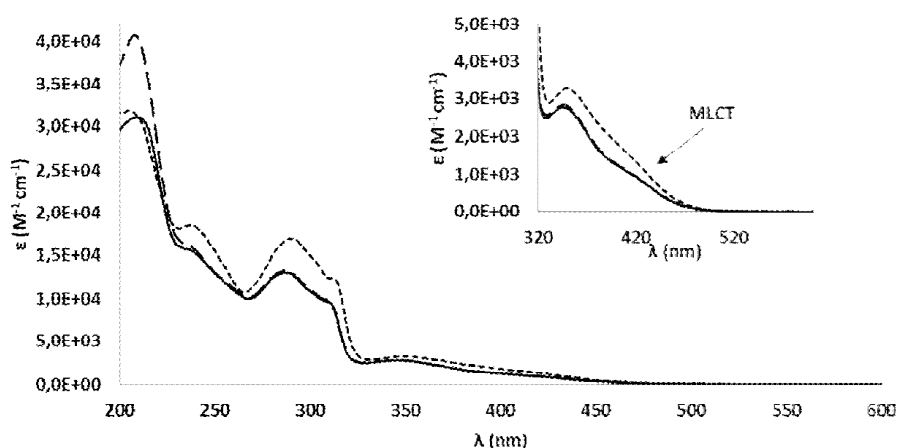

Fig. 1. Electronic spectra of [Ru^{II}(η^6-(2-phenoxyethanol))(bpy-R)Cl][PF$_6$] in acetonitrile solutions; - - - - **3**; —— **4**; − − **5**.

3.3. Single crystal structure of [Ru^{II}(η^6-(2-phenoxyethanol))(2,2'-bipyridine)Cl][PF$_6$] 3

[Ru^{II}(η^6-(2-phenoxyethanol))(bpy)Cl][PF$_6$] (**3**) crystallises as dark red prism (crystal dimensions 0.49 × 0.45 × 0.44 mm). Fig. 2 shows an ORTEP representation of [Ru^{II}(η^6-(2-

phenoxyethanol))(bpy)Cl]+ cation. In **3**, the asymmetric unit contains one cationic ruthenium complex and one PF_6^- anion. The Ru[II] centre adopts the pseudo-octahedral geometry, surrounded by a π-bonded arene from the phenoxyethanol. The bond distance Ru-arene [centroid, c1, 1.694(2) Å] is similar to other arene compounds containing other (N,N′)-chelating ligands [30]. The Ru-N bond distances between the nitrogen atoms of the pyridine rings of the ligand are nearly in the same range, 2.0694(15) Å and 2.0801(15) Å, as in other similar compounds with pyridine rings bonded [31]. The Ru−Cl bond distance is in the usual range. Strong intermolecular hydrogen bonds are present between the ethanol arms of arene ligand (see Table 1). π-π stacking lateral interactions are present in the crystal packing, which stabilize the structure. In Fig. 3, we can see the π-π stacking interactions between the centroids. The distances between the centroids are the same in all cases: d_{c1-c2} = 3.482(2) Å [c1 (C11J-C12J), c2 (C15D-C16D)]. These interactions and the strong intermolecular hydrogen bonds, between O(1) and O(2A or 2B), determine the disposition in chains in the crystal packing. Table 2 contains selected bond lengths and angles for the compound **3**.
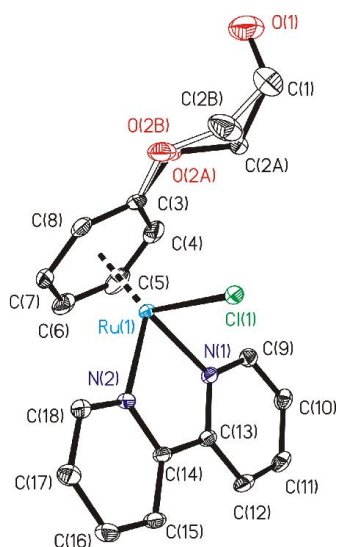

Fig. 2. ORTEP plot for [Ru[II](η⁶-(2-phenoxyethanol))(bpy)Cl]+ cation in compound **3**. All the non-hydrogen atoms are presented by their 50% probability ellipsoids. Hydrogen atoms are omitted for clarity.

Table 1. Hydrogen bonds in the compound **3** (bond lengths and angles)

D-H...A	d(D-H)	d(H...A)	d(D...A)	<(DHA)
O(1)-H(1)...O(2B)#1	0.82 Å	1.81 Å	2.570(13) Å	154.0 °
O(1)-H(1)...O(2A)#1	0.82 Å	2.26 Å	3.009(4) Å	152.9 °

Symmetry transformations used to generate equivalent atoms: #1 -x,-y+1,-z+1
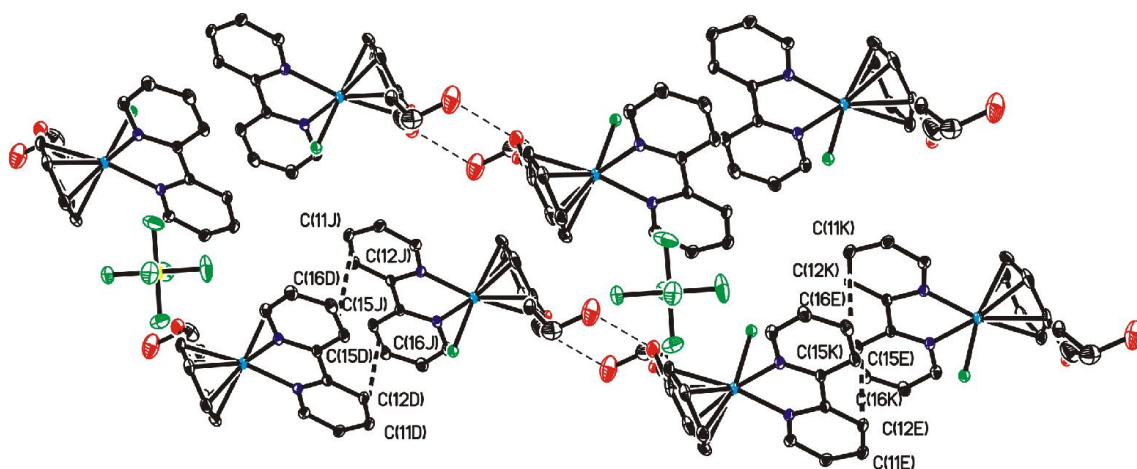
Fig. 3. View of crystal packing of compound **3**. π-π stacking lateral interactions and strong hydrogen bonds determine the disposition in chains.

Table 2. Bond lengths [Å] and angles [°] for complex **3.**

Bond lengths (Å)			
Ru(1)-N(1)	2.0694(15)	Ru(1)-C(5)	2.157(2)
Ru(1)-N(2)	2.0801(15)	Ru(1)-C(6)	2.194(2)
Ru(1)-Cl(1)	2.4031(5)	Ru(1)-C(7)	2.1885(19)
Ru(1)-C(3)	2.2685(19)	Ru(1)-C(8)	2.2191(19)
Ru(1)-C(4)	2.205(2)		
Angles (°)			
N(1)-Ru(1)-N(2)	77.27(6)	C(7)-Ru(1)-C(8)	37.27(7)
N(1)-Ru(1)-C(5)	90.32(7)	C(6)-Ru(1)-C(8)	67.83(8)
N(2)-Ru(1)-C(5)	129.93(8)	C(4)-Ru(1)-C(8)	67.57(8)

N(1)-Ru(1)-C(7)	143.24(7)	N(1)-Ru(1)-C(3)	132.27(7)
N(2)-Ru(1)-C(7)	94.42(7)	N(2)-Ru(1)-C(3)	149.38(7)
C(5)-Ru(1)-C(7)	67.53(8)	C(5)-Ru(1)-C(3)	66.83(9)
N(1)-Ru(1)-C(6)	108.01(7)	C(7)-Ru(1)-C(3)	66.79(7)
N(2)-Ru(1)-C(6)	101.10(8)	C(6)-Ru(1)-C(3)	79.12(8)
C(5)-Ru(1)-C(6)	37.24(9)	C(4)-Ru(1)-C(3)	36.78(9)
C(7)-Ru(1)-C(6)	37.77(8)	C(8)-Ru(1)-C(3)	37.35(8)
N(1)-Ru(1)-C(4)	100.78(7)	N(1)-Ru(1)-Cl(1)	86.28(4)
N(2)-Ru(1)-C(4)	167.62(8)	N(2)-Ru(1)-Cl(1)	84.67(4)
C(5)-Ru(1)-C(4)	37.70(10)	C(5)-Ru(1)-Cl(1)	143.44(7)
C(7)-Ru(1)-C(4)	79.78(8)	C(7)-Ru(1)-Cl(1)	129.08(6)
C(6)-Ru(1)-C(4)	67.64(9)	C(6)-Ru(1)-Cl(1)	165.39(6)
N(1)-Ru(1)-C(8)	168.34(7)	C(4)-Ru(1)-Cl(1)	107.50(7)
N(2)-Ru(1)-C(8)	113.96(7)	C(8)-Ru(1)-Cl(1)	97.56(5)
C(5)-Ru(1)-C(8)	80.02(8)	C(3)-Ru(1)-Cl(1)	89.07(6)

3.4. Electrochemical experiments

The redox response of the $Ru^{II}(\eta^6$-arene) moiety can be strongly influenced by the nature of the attached groups in the arene ligand [32]. Furthermore, the oxidation potentials of the Ru^{II} centres can be influenced by the different σ-donating and π-accepting capacities of the coordinated ligands [10,33]. To investigate such possible correlations in the present systems and to provide further characterization of the complexes, we performed an electrochemical study by cyclic voltammetry. The electrochemical responses of the complexes **2-5** were recorded at 200 mV/s, with a platinum disk working electrode in acetonitrile solutions containing tetrabutylammonium hexafluorophosphate as supporting electrolyte. **Table 3** summarizes the electrochemical data and Fig. 4 shows the cyclic voltammogram recorded for complex **3** as a representative example of the general electrochemical behaviour of the complexes.

The ligands bpy, 4,4'-dimethyl-2,2'-bipyridine and 4,4'-diyldimethanol-2,2'-bipyridine did not showed any electrochemical response between the experimental potential limits in acetonitrile.

Complex **2**, probably due to its cationic nature and the σ-donor ability of the acetonitrile ligands, was not found to be redox active in the acetonitrile solvent window towards the positive potentials range. However, in the negative potential range, this complex present a ligand based reduction process at −1.14 V.

The redox behaviour of the complexes **3-5** is fairly complicated due to the presence of consecutive and parallel chemical processes. Nevertheless, the overall reduction-oxidation pattern is similar for all the studied complexes. Upon scanning towards positive potentials, the complexes revealed an oxidation process for the Ru^{II} centre around +1.6 V without any counterpart reductive process observable upon back scanning. This behaviour indicates that the oxidized Ru^{III} compound is not stable and is involved in an electrode process with further chemical and electron-transfer reactions. The low stability is also detected in the shorter time scale of cyclic voltammetry, as shown in Fig. 4 in the case of complex **3**. Scan reversal following the Ru^{II}/Ru^{III} oxidation shows the appearance of two or three small reduction peaks at +0.88 V and +0.73 V respectively. The complexes also show ligand based irreversible reduction processes between −0.78 V and −1.55 V, followed of a small oxidation process between −0.58 V and −0.91 V in the reverse scan.

The values of the Ru^{II}/Ru^{III} oxidation potential of the studied complexes are expected to reflect the electron-donor character of their ligands, although the analysis has to be taken cautiously in view of the irreversible character of the oxidation waves. The electronic donor capacity of the hydroxyethoxy substituted arene ligand is known to be intermediate between that of benzene and *p*-cymene [34].

18

For the set of complexes with different substituents in the 3-position of the bpy ligand, the oxidation potentials follow the order: **3** > **5** > **4**. The Ru^{II} centre in complex **4** is easier oxidized than in **3** and **5**, indicating a higher electron density on the metal centre as consequence of the better electron σ-donor character of 4,4'-dimethyl-2,2'-bipyridine ligand.

Table 3. Electrochemical data of complexes **2-5** in acetonitrile *vs*. SCE (v = 200 mV/s)

Complex	E$_{pa}$ (V)	E$_{pc}$ (V)
2	---	−1.14
3	+1.66	---
	---	+0.88
	---	+0.73
	−0.72	−1.07
	---	−1.55
4	+1.54	---
	---	+0.81
	---	+0.67
	−0.81	−1.18
	---	−1.33
5	+1.62	---
	−0.63	−1.06
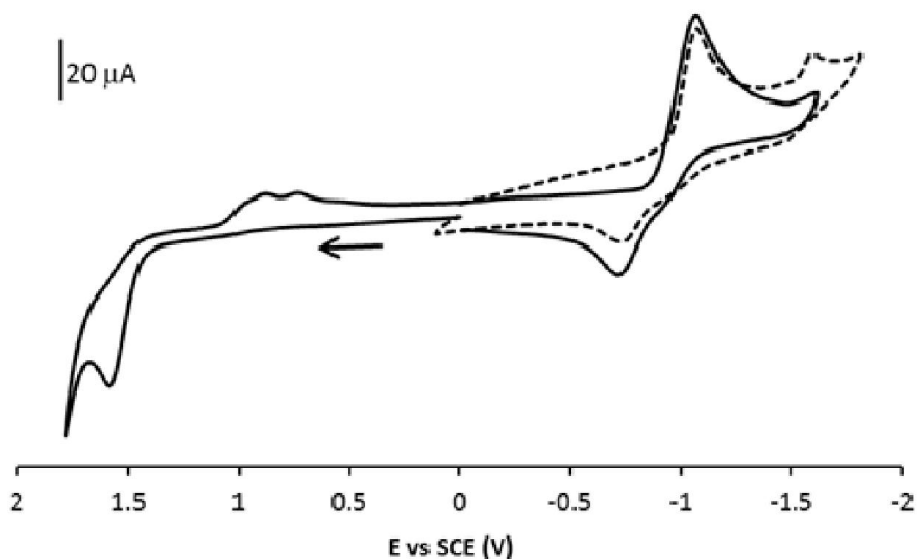
Fig. 4. Cyclic voltammogram of complex **3** in acetonitrile at a scan rate of 200 mV/s (the dashed line showed the reductive processes).

3.5. Speciation studies of [Ru^{II}(η^6-(2-phenoxyethanol))(bpy-R)Cl][PF$_6$] complexes in aqueous solution

Since in the Ru^{II}-arene compounds the metal-ligand (bpy-R) and the metal-chlorido bonds are relatively labile, diverse ligand exchange processes can take place in aqueous solutions. The most plausible changes are (i) replacement of the chlorido co-ligand by a water molecule, (ii) then the coordinated water can suffer deprotonation, and (iii) the metal ion can lose the bidentate ligand as well. These processes are affected by the acid-base properties of the ligands and the hydrolytic behaviour of the organometallic cation ([Ru^{II}(η^6-(2-phenoxyethanol))(H$_2$O)$_3$]$^{2+}$ in this case) as well. In order to comprehensively describe the solution equilibrium processes involving complexes **2-5** our work was initiated by hydrolytic studies of [Ru^{II}(η^6-(2-phenoxyethanol))Z$_3$] (MZ$_3$ where Z = H$_2$O or Cl$^-$) obtained by dissolving the precursor [Ru^{II}(η^6-(2-phenoxyethanol))(μ^2-Cl)Cl]$_2$ **1** in water (vide infra

20

Section 3.5.1). For a further understanding of the behaviour of our compounds **2-5**, and access their formation constants in chloride-containing media (mimicking the concentrations of the K$^+$, Na$^+$ and Cl$^-$ ions of the human blood serum), several experiments were carried out using [Ru^{II}(η^6-(2-phenoxyethanol))Z$_3$] solutions in the presence of the ligands, acetonitrile, bpy and its 4,4'-dimethyl- and 4,4'-diyldimethanol derivatives.

3.5.1 Hydrolytic processes of [Ru^{II}(η^6-(2-phenoxyethanol))(H$_2$O)$_3$]$^{2+}$ in the presence of chloride ions

The dissolution of the dimeric precursor [Ru^{II}(η^6-(2-phenoxyethanol))(μ^2-Cl)Cl]$_2$ (**1**) in water resulting in the formation of the monomeric species [Ru^{II}(η^6-(2-phenoxyethanol))Z$_3$] (MZ$_3$ where Z = H$_2$O or Cl$^-$) is assumed on the basis of the behaviour of analogous half-sandwich organometallic cations [38]. Its hydrolysis was studied by the combined use of UV–Vis and ^{1}H NMR titrations at 0.1 M ionic strengths (KCl), and we found that the equilibria could be reached fast (within 5-10 min) in the whole pH range studied (pH = 2–11.5). The overall stability constants for the various dinuclear hydrolysis products were determined by UV–Vis spectrophotometry and ^{1}H NMR spectra were recorded to confirm the speciation.

The pH dependent UV–Vis spectra in Fig. 5 show characteristic changes at pH > ~ 4.0 in the 230-500 nm wavelength range, which can be attributed to the hydrolysis of the [Ru^{II}(η^6-2-phenoxyethanol)Z$_3$] resulting in the formation of hydroxido-bridged dimers based on the analogy with other half-sandwich organometallics such as Ru^{II}-η^6-cymene [35] or Rh^{III}-η^5-pentamethylcyclopentadienyl complexes [36,37]. The dissimilar pH-dependence of the UV-Vis spectral changes at 430 and at 370 nm (see inset of Fig. 5) denotes the existence of at least one intermediate hydrolytic species. The spectra of the intermediate species display rather

similar characteristics to those of the complex formed at pH > 7, but are quite different from

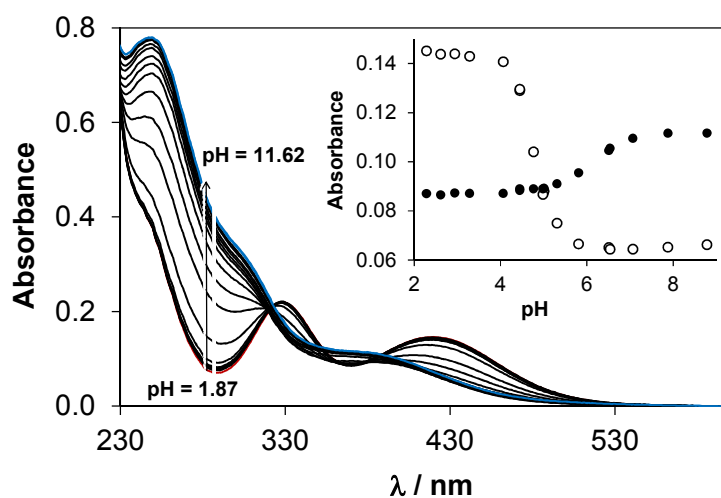those of $[Ru^{II}(\eta^6\text{-}(2\text{-phenoxyethanol}))Z_3]$.

Fig. 5. UV–Vis absorbance spectra of $[Ru^{II}(\eta^6\text{-}(2\text{-phenoxyethanol}))Z_3]$ at various pH values. Inset shows the changes of the absorbance values at 420 nm (○) and 370 nm (●) as function of the pH $\{c_M = 200\ \mu M;\ I = 0.1M\ (KCl);\ T = 25\ ^\circ C;\ Z = H_2O/Cl^-\}$.

In order to get a deeper insight into the formation of the intermediate species ^{1}H NMR spectra were recorded at various pH values (Fig. 6), which also refer to the presence of more than one kind of hydrolysis products. Firstly a triple peak set for the chemically equivalent *meta*-$(\eta^6\text{-}(2\text{-phenoxyethanol}))$ aromatic ring protons can be observed in the 5.8 – 6.4 ppm range at pH < 4.8. According to literature data chloride ions act as coordinating ligands, hence complexes such as $[Ru^{II}(\eta^6\text{-arene})(H_2O)_n(Cl)_{(3-n)}]^{(n-1)}$ (n = 3 or 2) or $[(Ru^{II}(\eta^6\text{-arene})_2(\mu^2\text{-}Cl)_3]^+$ were identified at acidic pH values [35]. In these species the water molecules can be partially or completely substituted by chlorido ligands depending on the concentration of the chloride ions [35]. The ^{1}H NMR spectra recorded for $[Ru^{II}(\eta^6\text{-}(2\text{-phenoxyethanol}))(H_2O)_3]^{2+}$ in the absence of chloride ions and in the presence of 3 M KCl support the formation of similar mixed aqua-chlorido complexes as well (Fig. S1). Thus the observed peaks in the low-

field region of the recorded ^{1}H NMR spectra in Fig. 6A can be attributed to the following species: *tris*-aqua complex (6.22 ppm), *mono*-chlorido complex (6.11 ppm) and *tris*-chlorido-bridged dimeric species (6.01 ppm) (see Fig. S1 and Table S2). These chemical shifts belong to the *meta*-(η^6-(2-phenoxyethanol)) aromatic ring protons. The doublets of the *ortho*-(η^6-(2-phenoxyethanol)) aromatic ring protons overlap with the triplet of *para*-(η^6-(2-phenoxyethanol)) aromatic ring proton, while the aliphatic protons are practically insensitive to the water/Cl$^-$ exchange processes in the coordination sphere.
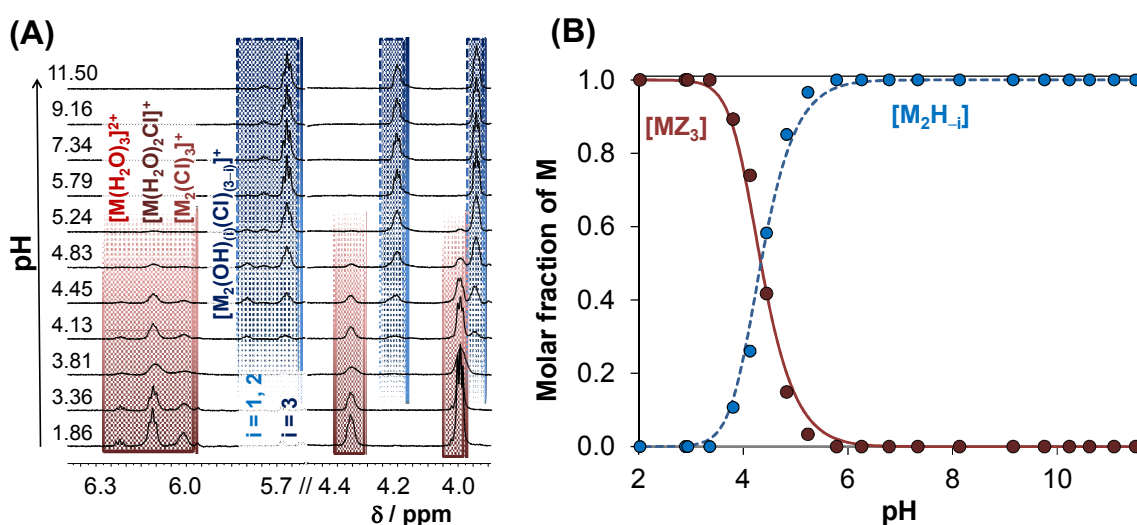
Fig. 6. pH-Dependent ^{1}H NMR spectra (A) and concentration distribution curves (B) of [Ru^{II}(η^6-(2-phenoxyethanol))Z$_3$] (MZ$_3$ where Z = H$_2$O or Cl$^-$) in the presence of 0.1 M KCl. Notations for ^{1}H NMR spectra: non-hydrolyzed species: [M(H$_2$O)$_3$]$^{2+}$, [M(H$_2$O)$_2$Cl]$^+$, [M$_2$(Cl)$_3$]$^+$ formed by water/Cl$^-$ exchange (solid frame); hydrolyzed species: [M$_2$(OH)Cl$_2$]$^+$, [M$_2$(OH)$_2$Cl]$^+$, [M$_2$(OH)$_3$]$^+$ formed by OH$^-$/Cl$^-$ exchange (dashed frame). Concentration distribution curves for [MZ$_3$] (solid line) and [M$_2$H$_{-i}$] hydroxido complexes (dashed line; i = 1, 2 or 3) calculated by the use of their overall stability constants, where M = Ru^{II}(η^6-(2-phenoxyethanol). Molar fractions based on the ^{1}H NMR peak integrals: [MZ$_3$] (●) and summarized fractions for the hydroxido complexes (■); M = Ru^{II}(η^6-(2-phenoxyethanol). {c_M = 2 mM; T = 25˚C; 10% D$_2$O}.

As reported in the literature, the hydrolysis of $[Ru^{II}(\eta^6\text{-arene})(Z)_3]^{2+}$ (Z = H_2O or Cl^-) results in the formation of various mixed chlorido/hydroxido-bridged intermediates with increasing pH in the chloride ion containing media such as complexes $[Ru^{II}(\eta^6\text{-arene})_2(\mu^2\text{-OH})_i(\mu^2\text{-Cl})_{(3-i)}]^+$ (i = 1–3) [35]. Accordingly, the intensity of the peak belonging to the mixed aqua-chlorido complexes $[Ru^{II}(\eta^6\text{-(2-phenoxyethanol))})(Z)_3]$ is decreasing with the increasing pH, and the appearance of a new multiple peak set at lower chemical shifts is seen at pH > ~3.8 (Fig. 6A). The molar ratio of the complexes belonging to the latter peaks alters in line with the increasing pH, and a single peak at 5.67 ppm becomes predominant at pH > 5.8. This latter finding indicated the formation of the *tris*-hydroxido dinuclear complex $[(Ru^{II}(\eta^6\text{-(2-phenoxyethanol)))})_2(\mu^2\text{-OH})_3]^+$ (denoted as $[M_2H_{-3}]$) which is formed in both the absence and the presence of chloride ions, as the chemical shift of this species is identical independently from the chloride content of the solvent (Fig. S1, Table S2).

Despite the fairly complicated speciation in the presence of chloride ions, the hydrolytic equilibrium processes can be well described assuming the formation of merely two kinds of hydroxido-bridged dimeric complexes such as $[M_2H_{-2}]$ and $[M_2H_{-3}]$ as in the case of other organometallic cations [38]. Therefore, the following overall stability constants were computed for the hydrolysis products of $[Ru^{II}(\eta^6\text{-(2-phenoxyethanol))})(Z)_3]$ at 0.1 M KCl: $\log\beta_{[M_2H_{-2}]} = -5.98 \pm 0.01$ and $\log\beta_{[M_2H_{-3}]} = -12.10 \pm 0.01$ based on the pH-dependent UV–Vis titrations. Concentration distribution curves were then calculated with the help of these stability constants according to the conditions used for the ^{1}H NMR titrations (Fig. 6B). The ^{1}H NMR signals of the non-hydrolysed and hydrolysed species were observed well separately in the case of the -OC**H**$_2$OH protons and their integrated values could be converted to molar

fractions of the metal ion. These values show a good agreement with the calculated data based on the UV–Vis spectrophotometric results (Fig. 6B).

Comparing the hydrolytic behaviour of complex $[Ru^{II}(\eta^6\text{-}(2\text{-phenoxyethanol}))(Z)_3]$ to that of analogous $[Ru^{II}(\eta^6\text{-}p\text{-cymene})Z_3]$ it can be concluded that the formation of hydrolysed species occurs in the same pH range at 0.1 M chloride ion content (Fig. S2). The summed concentration distribution curves for the p-cymene-containing complex were computed with combining the overall stability constants determined for the $[Ru^{II}(\eta^6\text{-}p\text{-cymene})(H_2O)_3]^{2+} - Cl^-$ system [35].

It is noteworthy that coordination of the ethanolic hydroxyl group of the aromatic cap to the Ru^{II}-centre cannot be excluded, however no evidence was found for the existence of this interaction.

3.5.2. Solution equilibria of $[Ru^{II}(\eta^6\text{-}(2\text{-phenoxyethanol}))Z_3]$ complexes of acetonitrile, 2,2'-bipyridine and its 4,4'-dimethyl- and 4,4'-diyldimethanol derivatives in chloride-containing media

The proton dissociation constant of ligand bpy was determined by pH-potentiometry formerly in our laboratory at I = 0.2 M KCl and KNO$_3$ [40]. The ligand bpy acts as a proton acceptor in acidic solutions (pK_a = 4.52 (KCl) and 4.41 (KNO$_3$)). The expected pK_a values of the 4,4'-dimethyl- and 4,4'-diyldimethanol derivatives are probably somewhat higher than that of bpy due to the presence of electron donating alkyl substituents. In case of acetonitrile no (de)protonation process was observed in the studied pH-range.

The solution stability of the complexes **[**$Ru^{II}(\eta^6\text{-}(2\text{-phenoxyethanol}))(NCCH_3)_2Cl][PF_6]$ **(2)** and $[Ru^{II}(\eta^6\text{-}(2\text{-phenoxyethanol}))(bpy\text{-}R)Cl][PF_6]$ **(3-5)** was investigated by the combined use of ^{1}H NMR and UV−Vis titrations in the presence of 0.1 M KCl.

The pH-dependent UV–Vis spectra of **2** were practically identical with those of $[Ru^{II}(\eta^6\text{-}(2\text{-}$phenoxyethanol))Z_3]$, which clearly indicates that the complex decomposes in aqueous solution in the pH range 2.0–11.5. ^{1}H NMR measurements also confirmed this finding (see Fig. S3).

The complex formation process in case of the complexes of bpy-R is rather slow: the equilibrium could be reached within 30–40 min after mixing $[Ru^{II}(\eta^6\text{-}(2\text{-phenoxyethanol})Z_3]$ and bpy at pH 3.0. Although no complex formation was observed within 3 h at pH 10.0, only the summed spectra of the dimeric hydroxido complex $[(Ru^{II}(\eta^6\text{-}(2\text{-phenoxyethanol})))_2(\mu^2\text{-}OH)_3]^+$ and the free bpy could be observed in solution. This later conflicts the thermodynamically expected behaviour (*i.e.* formation of $[ML(OH)]^+$ and subsequent oxidation of it, vide infra, which can be explained by the assumed high kinetic inertness of the *tris*-hydroxido-bridged Ru^{II}-species [23].

The stability of the complex **3** is significantly high, as no decomposition was observed on the basis of the UV–Vis spectra even at fairly low pH (pH = 1.0), therefore only a threshold could be computed for the stability constant of **3** that denotes a $\log\beta_{[ML]} \geq 11.0$ (where we assume that < 3% spectral change cannot be detected). The predominant species is the $[Ru^{II}(\eta^6\text{-}(2\text{-}$phenoxethanol))(bpy)Z]$ up to pH 6.0. ^{1}H NMR spectra showed no dissociation of the complex within 2 days in the pH range 2.0-6.0 as well. Multiple processes take place at pH values > 6. Most probably the deprotonation of the coordinated water molecule or the substitution of chlorido co-ligand by a hydroxido in the position "Z" starts leading to the formation of species $[ML(OH)]^+$, which seems to be a relatively slow process (> 2 h). Unfortunately, in addition to this reaction other overlapping spectral changes were observed; and no pK_a for [MLZ] could be calculated. Namely, the novel process leads to the development of intensive absorption bands at 470 and 580 nm in the UV–Vis spectra, and the

pale yellow colour of the samples turned into greyish-green or -pink, which denotes quite extreme changes regarding the structure and/or the oxidation state of the original complex (Fig. 7).
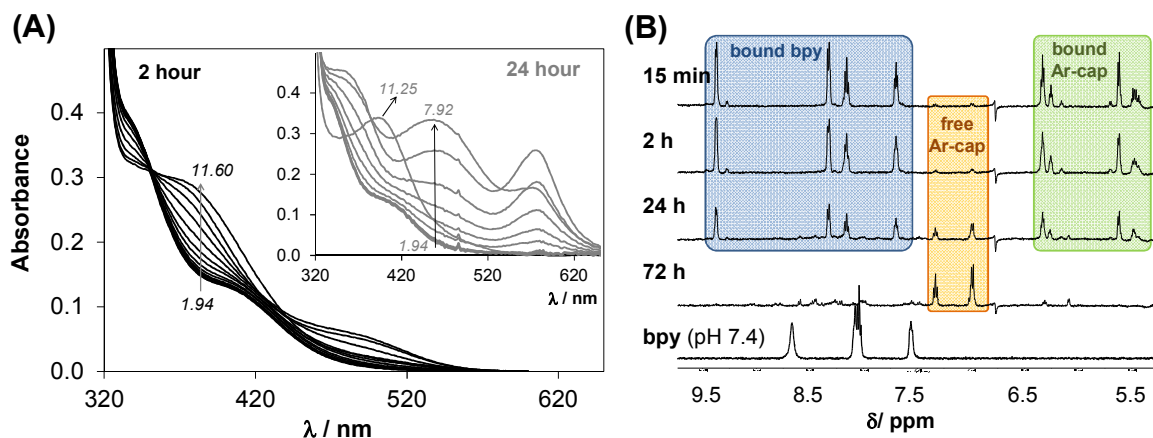

Fig. 7. UV–Vis absorbance spectra of $[Ru^{II}(\eta^6\text{-(2-phenoxyethanol)})(bpy)Z]$ **3** at various pH values after 2 h incubation, *inset* shows the spectra after 24 h (A); and time dependent ^{1}H NMR spectra of the same system followed at pH 7.4 (PBS') (B) {$c_{complex}$ = 267 μM (UV–Vis) or 1 mM (NMR); c_{bpy} = 2 mM (NMR); I = 0.1M (KCl); T = 25 ℃; Z = H_2O/Cl^-} (Ar-cap = 2-phenoxyethanol).

In order to get a deeper insight into the structure of the formed new species time dependent ^{1}H NMR spectra were recorded for **3** at pH 7.4. The spectral changes in Fig. 7B clearly show the decomposition of the initially predominant complex $[Ru^{II}(\eta^6\text{-(2-phenoxyethanol)})(bpy)Z]$, but instead of the release of bpy, free 2-phenoyethanol occurs and signals belonging to bpy protons disappear gradually. This observation refers to the oxidation of the Ru^{II}-centre to Ru^{III}, which results in the loss of its arene ligand but not bpy. The ^{1}H NMR signals of bpy cannot be detected owing to their paramagnetic shifting and/or broadening. It should be noted, that in the presence of 1 M KCl complex **3** showed no dissociation within 24 h at pH 7.4, which suggests that formation of $[ML(OH)]^+$ (that is suppressed in the presence of chloride ions) is the initial step of the oxidation process. Partial loss of the arene ligand was also

reported for $[Ru^{II}(\eta^6\text{-biphenyl})(L)Cl]$ complexes where L = bpy or 3,3'-hydroxy-bpy during the aquation, however no pH-range is indicated in this paper for the process [41]. While the analogous bpy complex of $Rh^{III}(\eta^5\text{-}C_5Me_5)$ was found to have considerably high stability in a wide pH range [39].

Since most probably an oxidation reaction takes place in the case of complex **3**, samples were carefully deoxygenized by argon purging and UV–Vis spectral changes were followed at pH 7.4. However, the assumed oxidation took place in the same manner as in case of samples kept in normal aerobic conditions. The oxidation seems to be a slow process; no equilibrium could be reached even after 1 week. The pH influences the rate and the quality of the product formed as well. Fig. 8 shows the spectral changes of two samples followed at pH 8.02→7.88 and 9.58→9.05 respectively. The pH values connected with arrows indicate the decrease of the pH in course of the experiment, which could not be avoided. Characteristic bands appeared at 380 nm, 470 nm and 580 nm on the spectra followed at pH ~8 (Fig. 8A); and the same behaviour was found at pH ~7. However at pH ~9.5 (Fig. 8B) and at pH ~10 only one intensive band at 470 nm was developed. Time dependence of these processes at various pH values is presented in Fig. 9. It can be seen that the fastest changes happen between pH 8 and 9.5, however a direct comparison (*i.e.* calculation of rate constants) is not allowed since the forming products are not identical at the certain pH values. Remarkably no oxidation was observed at pH ≤ 6 and pH ≥ 11 based on UV–Vis and ^{1}H NMR measurements. Samples contain the complex in its [MLZ] form at pH ≤ 6, while the slow (~ 24 h) formation of $[ML(OH)]^+$ at pH ≥ 11 is probable and no free bpy or hydroxido-bridged dimers occur here (see Fig. S4).
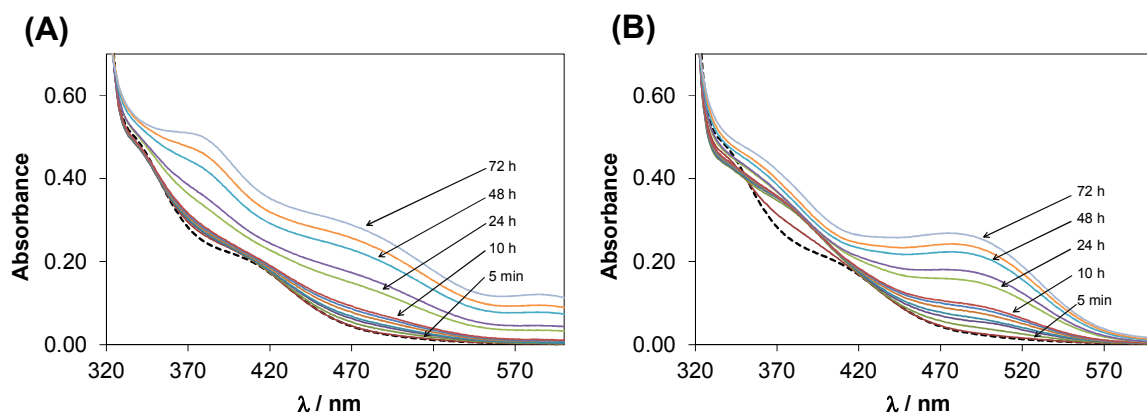
Fig. 8. Time dependent UV–Vis absorbance spectra of $[Ru^{II}(\eta^6\text{-}(2\text{-phenoxyethanol}))(bpy)Z]$ at pH $8.02{\rightarrow}7.88$ (A) and $9.58{\rightarrow}9.05$ (B) $\{c_{complex} = 195\ \mu M;\ I = 0.1M\ (KCl);\ T = 25\ ^{\circ}C;\ Z = H_2O/Cl^-\}$.
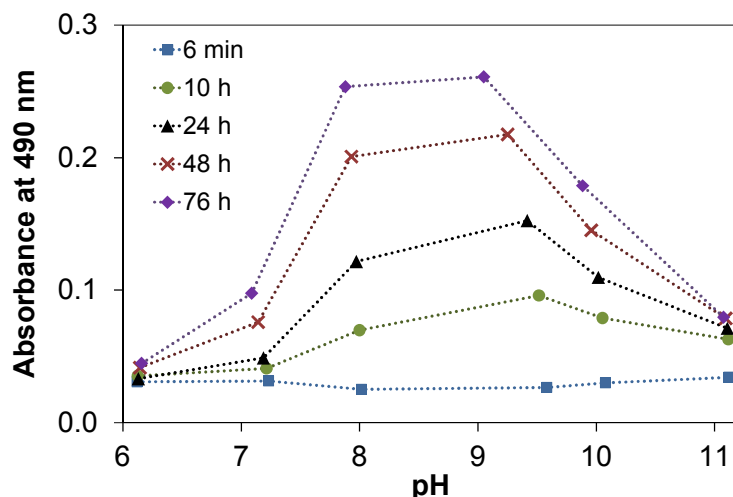

Fig. 9. Changes of the absorbance of $[Ru^{II}(\eta^6\text{-}(2\text{-phenoxyethanol}))(bpy)Z]$ at 490 nm followed between pH 6 and 11 using different incubation periods (6 min −76 h). $\{c_{complex} = 195\ \mu M;\ I = 0.1M\ (KCl);\ T = 25\ ^{\circ}C;\ Z = H_2O/Cl^-\}$.

The 4,4'-dimethyl- (**4**) and 4,4'-diyldimethanol (**5**) derivatives displayed similar behaviour compared to **3**. The [MLZ] complex is already predominant at pH 2.0, most likely the stability of these complexes is somewhat higher than that of **3**. The oxidation starts only at pH > 7.0,

which supports the former assumption as well. At pH 11.5, neither the formation of $[ML(OH)]^+$ or additional oxidation was detected for both complexes.

In the species $[Ru^{II}(\eta^6\text{-(2-phenoxyethanol)})(L)Z]$ the third coordination site (Z) is most probably occupied by a water molecule in the absence of chloride ions, although it can be partially (or completely) displaced by a chlorido ligand in a chloride containing milieu, or *vice versa,* the originally chlorinated complex can suffer aquation after dissolution. The coordination of the labile chlorido results in characteristic spectral changes in the UV–Vis spectra of the complexes (Fig. S5), therefore the equilibrium constants (log $K'(H_2O/Cl^-)$) could be estimated for the $[Ru^{II}(\eta^6\text{-(2-phenoxyethanol)})(L)(H_2O)]^+ + Cl^- \rightleftharpoons [Ru^{II}(\eta^6\text{-(2-phenoxyethanol)})(L)(Cl)] + H_2O$ equilibrium at pH values (~ 5) where complexes $[Ru^{II}(\eta^6\text{-(2-phenoxyethanol)})(L)Z]$ are predominate (Table 4). The computed equilibrium constants represent considerably high affinity of the complexes towards chloride ions. According to the H_2O/Cl^- exchange constants it can be noted that at pH ~ 5, $\sim 95\%$ and 83% of the bpy complex (**3**) is chlorinated at 100 and 24 mM chloride concentrations of the serum and the intracellular fluid, respectively.

Table 4. Aqua-chlorido exchange constants for the $[Ru^{II}(\eta^6\text{-(2-phenoxyethanol)})(L)Z]$ complexes determined by UV–Vis at pH = 4.9–5.2 and at various concentrations of chloride ions $\{T = 25\,°C; I = 0.1\ M\ (KCl);\ Z = H_2O\ /\ Cl^-\}$.

Complex	log$K'(H_2O/Cl^-)^{a}$
3	2.31(1)
4	2.20(1)
5	2.41(1)

[a] Standard deviations (SD) are in parenthesis

4. Conclusions

Three new piano-stool ruthenium(II) compounds with the general formula $[Ru^{II}(\eta^6$-(2-phenoxyethanol))(bpy-R)Cl][PF$_6$] were synthesized and fully characterized. The structure of $[Ru^{II}(\eta^6$-(2-phenoxyethanol))(bpy)Cl][PF$_6$] (**3**) was further characterized in solid state by single-crystal X-ray diffraction analysis. Complex **3** crystallizes in the monoclinic P2$_{1/c}$ space group and adopts a pseudo octahedral geometry. The strong π-π stacking lateral interactions in the crystal packing stabilizes the structure. The oxidation potentials for this set of Ru^{II} compounds was related to the σ-donating ability of the coordinated ligand, being complex **4** with the 4,4'-dimethyl-2,2'-bipyridine substituent the most readily oxidized.

The solution equilibrium behaviour of the structured half-sandwich Ru^{II}-arene derivatives, namely $[Ru^{II}(\eta^6$-(2-phenoxyethanol))Z$_3$] (=MZ$_3$) parent compounds and its complexes formed with bidentate (N,N)-donor containing ligands (bpy-R) was also investigated in presence of 0.1 M chloride ions (mimicking the concentration in human blood serum). The $[Ru^{II}(\eta^6$-(2-phenoxyethanol))Z$_3$] species hydrolyses reversibly and formation constants for the dimeric hydroxido complexes $[M_2(\mu$-OH)$_3]^+$ and $[M_2(\mu$-OH)$_2$Z$_2]$ (Z = H$_2$O/Cl$^-$) are reported. The monodentate *bis*-acetonitrile complex (**2**) decomposes immediately after dissolution in water. Exclusive formation of mono-ligand complexes ([MLZ]) with considerable high stability could be detected in the case of the bpy and its derivatives possessing (N,N) donor set. No significant difference between the complex stabilities of the three derivatives (bpy, 4,4'-dimethyl-bpy, 4,4'-diyldimethanol-bpy) was observed. Water–chloride exchange equilibrium in the [ML(H$_2$O)]$^+$ complexes was also studied by UV–Vis spectrophotometry at pH 5. Based on the constants it can be predicted that, *e.g.* ~95% of the bpy complex is chlorinated at 0.1 M chloride ion concentration representing a fairly strong affinity towards this halide anion. At the same time none of these complexes (**3**–**5**) is stable at physiological pH (pH 7.4) and

31

multiple hydrolytic and oxidation processes take place, and the rate of the oxidation and the structure of the final product depend on the pH. This behaviour of the studied Ru^{II} complexes hindered further biological studies, which points out the need for the elucidation of the aqueous solution chemistry of potentially active metal complexes prior to their *in vitro* bio assays.

Appendix. Supplementary data

Supplementary data related to this article can be found online at…

References

[1] W.M. Motswainyana, P.A. Ajibade, Advances in Chemistry (2015) article ID 859730.

[2] T.J.L. Silva, P.J. Mendes, T.S. Morais, A. Valente, M.P. Robalo, M.H. Garcia, in: G.P. Keeler (Ed.), Ruthenium: Synthesis, Physicochemical Properties and Applications, Nova Science Publishers, Inc., N.Y., USA, 2014, pp.105–164.

[3] A.M. Pizarro, A. Habtemariam, P.J. Sadler, Top Organomet. Chem. 32 (2010) 21–56.

[4] A. Amin, M.A. Buratovich, Med. Chem. 9 (2009) 1489–1503.

[5] A. Valente, M.H. Garcia, Inorganics 2 (2014) 96–114.

[6] V. Moreno, M. Font-Bardia, T. Calvet, J. Lorenzo, F.X. Alvilés, M.H. Garcia, T.S. Morais, A. Valente, M.P. Robalo, J. Inorg. Biochem. 105 (2011) 241–249.

[7] T.S. Morais, T.J.L. Silva, F. Marques, M.P. Robalo, F. Avecilla, P.J.A. Madeira, P.J.G. Mendes, I. Santos, M.H. Garcia, J. Inorg. Biochem. 114 (2012) 65–74.

[8] T.S. Morais, F. Santos, L. Côrte-Real, F. Marques, M.P. Robalo, P.J.A. Madeira, M.H. Garcia, J. Inorg. Biochem. 122 (2013) 8–17.

[9] T.S. Morais, F.C. Santos, T.F. Jorge, L. Côrte-Real, P.J.A. Madeira, F. Marques, M.P. Robalo, A. Matos, I. Santos, M.H. Garcia, J. Inorg. Biochem. 130 (2014) 1–14.

[10] L. Côrte-Real, M.P. Robalo, F. Marques, G. Nogueira, F. Avecilla, T.J.L. Silva, F.C. Santos, A.I. Tomaz, M.H. Garcia, A. Valente, J. Inorg. Biochem. 150 (2015) 148–159.

[11] W.H. Ang, P.J. Dyson, Eur. J. Inorg. Chem. (2006) 4003–4018.

[12] C. Scolaro, A. Bergamo, L. Brescacin, R. Delfino, M. Cocchietto, G. Laurenczy, T.J. Geldbach, G. Sava, P.J. Dyson, J. Med Chem. 48 (2005) 4161–4171.

[13] A. Bergamo, A. Masi, A.F. Peacock, A. Habtemariam, P.J. Sadler, G. Sava, J. Inorg. Biochem. 104 (2010) 79–86.

[14] Y.K. Yan, M. Melchart, A. Habtemariam, P.J. Sadler, Chem. Commun. (2005) 4764–4776.

[15] T. Bugarcic, A. Habtemariam, R.J. Deeth, F.P.A. Fabbiani, S. Parsons, P.J. Sadler, Inorg. Chem. 48 (2009) 9444–9453.

[16] Y. Zhang, W. Zheng, Q. Luo, Y. Zhao, E. Zhang, S. Liua, F. Wang, Dalton Trans. 44 (2015) 13100–13111.

[17] K. Ghebreyessus, A. Peralta, M. Katdare, K. Prabhakaran, S. Paranawithana, Inorg. Chim. Acta 434 (2015) 239–251.

[18] R.A. Delgado, A. Galdamez, J. Villena, P.G. Reveco, F.A. Thomet, J. Organomet. Chem. 782 (2015) 131–137.

[19] P.C.A. Bruijnincx, P.J. Sadler, Adv. Inorg. Chem. 61 (2009) 1–62.

[20] S.J. Dougan, M. Melchart, A. Habtemariam, S. Parsons, P.J. Sadler, Inorg. Chem. 45 (2006) 10882−10894.

[21] R.E. Morris, R.E. Aird, P. del S. Murdoch, H. Chen, J. Cummings, N.D. Hughes, S. Parsons, A. Parkin, G. Boyd, D.I. Jodrell, P.J. Sadler, Med. Chem. 44 (2001) 3616–3621.

[22] M. Melchart, A. Habtemariam, O. Novakova, S.A. Moggach, F.P.A. Fabbiani, S. Parsons, V. Brabec, P.J. Sadler, Inorg. Chem. 46 (2007) 8950−8962.

[23] F. Wang, H. Chen, S. Parsons, I.D.H. Oswald, J.E. Davidson, P.J. Sadler, Chem. Eur. J. 9 (2003) 5810–5820.

[24] D.D. Perrin, W.L.F. Amarego, D.R. Perrin, Purification of Laboratory Chemicals, 2nd Ed., Pergamon, New York, 1980, pp. 65–371.

[25] J. Soleimannejad, C. White, Organometallics 24 (2005) 2538–2541.

[26] J. Soleimannejad, H. Adams, C. White, Anal. Sci.: X-Ray Struct. 21 (2005) x151–x152.

[27] G.M. Sheldrick, SADABS (Version 2.10), University of Göttingen, Germany, 2004.

[28] G.M. Sheldrick, Acta Crystallogr. Sect. A 64 (2008) 112–122.

[29] L. Zékány, I. Nagypál, in: D.L. Leggett (Ed.), Computational Methods for the Determination of Stability Constants, Plenum Press, New York, 1985, pp. 291–353.

[30] M. Martínez-Alonso, N. Busto, F.A. Jalón, B.R. Manzano, J.M. Leal, A.M. Rodríguez, B. García, G. Espino, Inorg. Chem. 53 (2014) 11274–11288.

[31] T. Tsolis, M.J. Manos, S. Karkabounas, I. Zelovitis, A. Garoufis, J. Organomet. Chem. 768 (2014) 1–9.

[32] M. Auzias, B. Therrien, G. Suss-Fink, P. Stepnicka, W.H. Ang, P.J. Dyson, Inorg. Chem. 47 (2008) 578–583.

[33] L.C. Matsinha, P. Malatji, A.T. Hutton, G.A. Venter, S.F. Mapolie, G.S. Smith, Eur. J. Inorg. Chem. 24 (2013) 4318–4328.

[34] B. Lastra-Barreira, J. Díez, P. Crochet, Green Chem. 11 (2009) 1681–1686.

[35] L. Bíró, E. Farkas, P. Buglyó, Dalton Trans. 41 (2012) 285-291.

[36] O. Dömötör, S. Aicher, M. Schmidlehner, M.S. Novak, A. Roller, M.A. Jakupec, W. Kandioller, C.G. Hartinger, B.K. Keppler, E.A. Enyedy, J. Inorg. Biochem. 134 (2014) 57–65.

[37] M.S. Eisen, A. Haskel, H. Chen, M.M. Olmstead, D.P. Smith, M.F. Maestre, R.H. Fish, Organometallics 14 (1995) 2806–2812.

[38] L. Bíró, A.J. Godó, Z. Bihari, E. Garribba, P. Buglyó, Eur.J. Inorg. Chem. 17 (2013) 3090–3100.

[39] S. Ohkuma, B. Poole, Proc. Natl. Acad. Scd. USA 75 (1978) 3327–3331.

[40] E.A. Enyedy, J.P. Mészáros, O. Dömötör, C.M. Hackl, A. Roller, B.K. Keppler, W. Kandioller, J. Inorg. Biochem. 152 (2015) 93–103.

[41] T. Bugarcic, A. Habtemariam, J. Stepankova, P. Heringova, J. Kasparkova, R.J. Deeth, R.D.L. Johnstone, A. Prescimone, A. Parkin, S. Parsons, V. Brabec, P.J. Sadler, Inorg. Chem. 47 (2008) 11470–11486.